

# Shoreline Changes and Sediment Distribution Studies for India's West Coast



Kavitha Natarajan, P. K. Suresh, and R. Sundaravadivelu

**Abstract** The study investigates the rate of erosion and accretion on shorelines along the West Coast of Gulf of Combat, Gujarat, India. GoC is selected for the study falls within the latitudes and longitudes of  $20^{\circ} 56' 31''$  to  $21^{\circ} 17' 25''$  and  $72^{\circ} 2' 18''$  to  $72^{\circ} 49' 55''$  with a coastal length of 276 km. The objective was accomplished through the use of remote sensing and GIS techniques, and 45 years of shoreline data were used for the analysis between 1973 and 2017. Landsat multispectral images-enhanced thematic mapper LISS III & LISS IV data covering the period of 12 years between 2005, 2011, 2014, and 2017 and was used for the Thapi coast. Net shoreline movement (NSM) and end point rate (EPR) were calculated using ArcGIS-DSAS computing statistical methods. DSAS calculates the change metrics by measuring the distance between the baseline and each shoreline intersection along a transect and combining date (year) information and positional uncertainty for each shoreline. Transport of sediment: According to the findings of the NSM study, the accretion rate is greater than the erosion rate. Between 1973 and 2005, erosion and accretion were approximately 0.6 km and 53.9 km, respectively. From 2005 to 2011, the erosion rate was 0.2, with an accretion of 38.7 km. For the years 2011 to 2014, erosion and accretion had no notable values; both rates were 2 km. For the years 2014–2017, erosion and accretion are approximately 0.6 km and 2.8 km. According to EPR findings, the erosion rate (-1.30 km/year) and accretion rate (3.60 km/year) between 2005 and 2011 are higher than in preceding years. The rate of erosion is slightly higher for the years 2005 to 2011 (- 1.30 km/year), and then, it falls to - 0.7 km/year (2011–2014) and - 10.2 km/year after that (2014–2017). Results of accumulation show that the rate was high, with a value of 3.6 km/year, for the

---

K. Natarajan  
GIS Specialist, TNIAMP, WRD, Chepauk, Chennai 600005, India

P. K. Suresh (✉)  
Meenakshi Sundararajan Engineering College, Kodambakkam, Chennai 600024, India  
e-mail: [sureshpk2000@gmail.com](mailto:sureshpk2000@gmail.com)

R. Sundaravadivelu (✉)  
Department of Ocean Engineering, Indian Institute of Technology, Madras, Chennai 600036, India  
e-mail: [rsun@iitm.ac.in](mailto:rsun@iitm.ac.in)

years 2005–2011. Then, it displays a declining tendency for the years 2011–2014 and 2014–2017, with a value of 0.6 km/year.

**Keywords** Sediment · Shoreline changes · RS · GIS-DSAS

## 1 Introduction

Coastal landforms are dynamic systems that function over a range of temporal and spatial scales. Dominant physical factors such as wave height, wave energy, tidal range, and littoral drift are responsible for shaping coastal landforms [1]. Multi-dated satellite images can be used to monitor shoreline changes by measuring sedimentation, erosion, and accretion [2]. Seasonal variations in wave energy, wave height, and wave direction have resulted in asymmetric shoreline erosion by altering sediment movement trends in the near shore area [3–6]. In the assessment of shoreline change, Landsat MSS, TM, ETM, and spot imagery have produced consistent results [7]. For the purposes of coastline extraction, assessment of erosion and accretion, and coastal morphology change detection at local and regional scale, numerous authors have exploited multi-temporal satellite imagery [8, 9].

The shorelines extracted from multi-temporal Landsat TM and ETM images were analyzed with DSAS software to determine the rate of erosion and retreating along the coastal area [10]. United States Geological Survey (USGS) developed Digital Shoreline Analysis System (DSAS) software, an add-on tool to ArcGIS used for the statistical analysis to compute the shoreline rate of change. The linear regression rate (LRR) and end point rate (EPR) statistics were used to identify the eroding, accreting, and stable shoreline for the study area [11].

According to current information by the Ministry of Earth Sciences (MoES), of the 6907 km of Indian coastline, about 34% is eroding, 26% is accreting, and the remaining 40% is constant. National Centre for Coastal Research (NCCR), which is part of the MoES, has been keeping an eye on coastline erosion since 1990 and it is continuously monitored using GIS and RS from 1990 to 2018. Rate of erosion of Gujarat (1946 km)—27%, Tamil Nadu (991 km)—43%, Kerala (593 km)—46%, West Bengal (534 km)—60%, and Puducherry (42 km)—23% make up the major coastal status for the years 1990–2018 [12]. The West Coast of India stretches from north to south and is comprised of the I Konkan, (ii) Karnataka, and (iii) Kerala coasts. It stretches from the Gulf of Cambay (Gulf of Khambhat) in the north to Cape Comorin (Kanniyakumari); on this, the two main estuaries in this strip are the Narmada and Tapi. In Gulf of Cambay (GoC), a large tidal range during high and low tides gives rise to strong tidal currents and develops a mechanism of sediment transportation. Interestingly, the inverted funnel shape of GoC has largely contribute to the sediment deposition in this region. During high tide, the tide currents move into the Gulf and encroaches the river mouth, whereas during low tide, they move out. This regular phenomena since long period on geological time scale has modified the geomorphological features in this region [13].

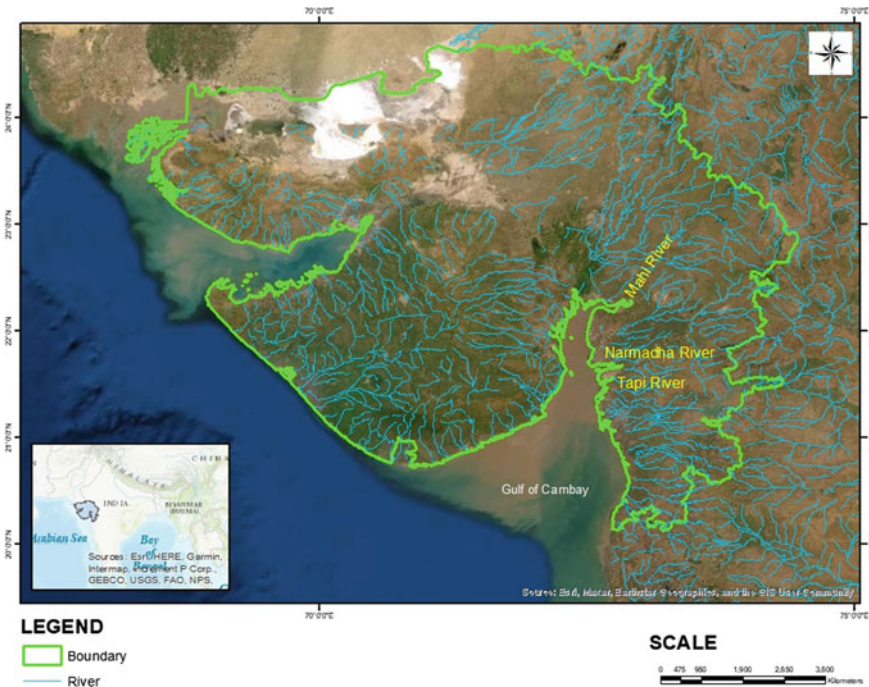


Fig. 1 Location map of the study area

## 2 Study Area

Due to its significance and highly influenced by the tidal currents other than geological and structural setup, the GoC is selected for the study within the latitudes and longitudes of 20° 56' 31" to 21° 17' 25" and 72° 2' 18" to 72° 49' 55" (Fig. 1) with a coastal length of 276 km. The South Gujarat coast trending almost north to south which is uniform and broken for few indentations. The major rivers traversing are Tapi and Mindhol. The following are the primary goals of the remote sensing and GIS research:

- To identify changes in the Tapi River estuary region
- To quantify the rate of erosion and identify the sediment distribution pattern

## 3 Materials and Method

The above goal was accomplished through the use of remote sensing and GIS techniques, 45 years of shoreline data were used for the analysis, base data was taken from the SOI toposheet, and the other's remote sensing data was used. For calculating

the rate of sediment transport analysis, digital shoreline analysis system (DSAS) method was adopted. The US Geological Survey created the DSAS arc map extension (USGS). DSAS works better in analyzing shoreline change and observing specific damaged sites in smaller areas, whereas the latest remote sensing techniques with geographic information system (GIS) have proven to be very useful in monitoring coastline changes and more effective in terms of both cost and time than conventional techniques. To obtain data and results, the DSAS system requires some shoreline from various dates. Some researchers are employing the device, which incorporates several shoreline DSAS with both long- and short-time scales. The primary goal of this research is to compare the changes in shoreline that occur within the study area. The two coastlines and five shorelines are combined using DSAS to identify and measure erosion and accretion. The GIS layers of multi-date shorelines were used as input for the DSAS model to calculate the rate of change over a 45-year period from 1972 to 2017 [14].

The Survey of India (SOI) Topographical maps were used as base map and was georeferenced using its latitude and longitudinal values of the 4 corners and projected as geographic WGS 84 and for the area calculation purpose further projected as UTM Zone 43° North. Using the visual interpretation techniques [15], HTL and LTL maps were prepared on 1:50,000 scale for the year 1972. In similar way, the remote sensing products were georeferenced using this rectified topo sheet, and shoreline maps were prepared for the year for various years (Table 1). Landsat multispectral images-enhanced thematic mapper LISS III & LISS IV data covering the period of 12 years between 2005, 2011, 2014, and 2017 and was used for the Thapi coast (Fig. 2). Erdas imagine software was used for Raster Analysis and ArcGIS 10.1 software used for vector analysis.

The US Geological Survey's (USGS) arc map extension compatibility DSAS was used to analyze shoreline changes. Net shoreline movement (NSM) and end point rate (EPR) were calculated using ArcGIS-DSAS computing statistical methods. DSAS calculates the change metrics by measuring the distance between the baseline and each shoreline intersection along a transect and combining date (year) information and positional uncertainty for each shoreline. NSM was used for distance measurement, and EPR was used for statistical analysis:

**NSM:** Net shoreline change measured by distance rather than mean value. NSM refers to the date, and only two shorelines are required, i.e., the total distance between the earliest and latest shoreline in each transect.

**Table 1** .

S. No.	Data type	Sensor	Year	Resolution (m)	Bands
1	Landsat 7	ETM +	2005	30	8
2	IRS 1C	LISS III	2011	23.5	4
3	Resourcesat 2	LISS III	2014	23.5	4
4	Resourcesat 2	LISS IV	2017	5.8	3

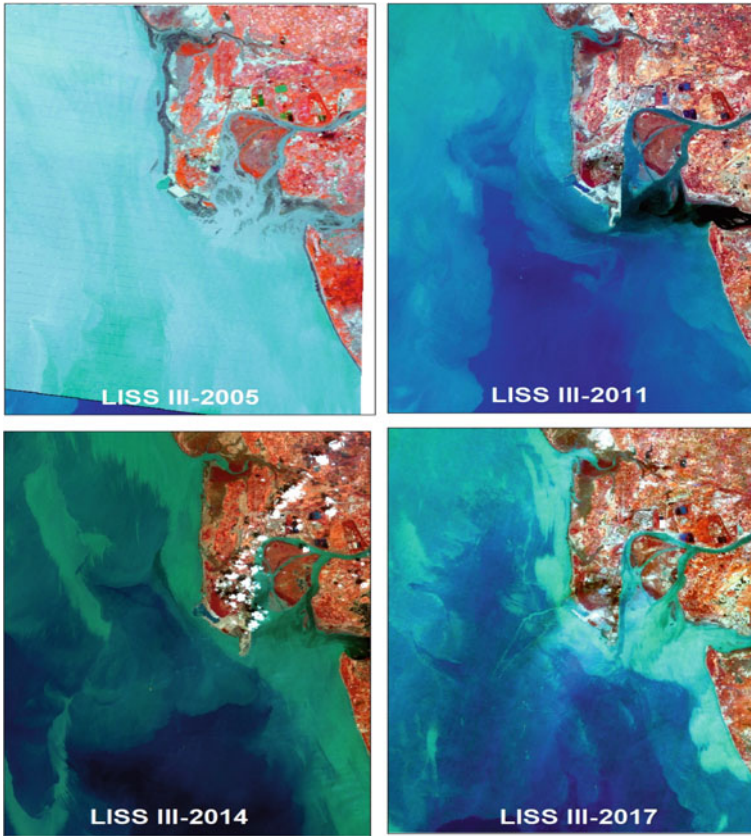


**Fig. 2** Remote sensing data for the year 2005, 2011, 2014 & 2017

**EPR:** It is calculated by dividing the distance between the oldest and youngest shorelines by the time elapsed between them [14].

The SOI 1972 data was used to establish the baseline. A buffer of 300 m was built to the baseline's left and right (toward land and sea directions). Baselines were chosen based on the dominant change direction and in parallel with the general shoreline orientation, and 138 transect lines were established at 20 m intervals along the entire coastline. The detailed methodology was shown in (Fig. 3). The seaward shift of the shoreline along the transect is considered a positive value (accretion) based on the position with reference to the baseline at each transect, while the landward shift is considered a negative value (decrement) (erosion). Two main statistical modules, NSM and EPR, are used among the various computational functions to measure the rate of change for a time series of shoreline layers [16]. The NSM is used to calculate the rate of change between 1972 and 2017 shorelines at each transect intersecting point, and the EPR is used to estimate the per year rate of change between the same periods. This is accomplished by dividing the distance of NSM at specific transects

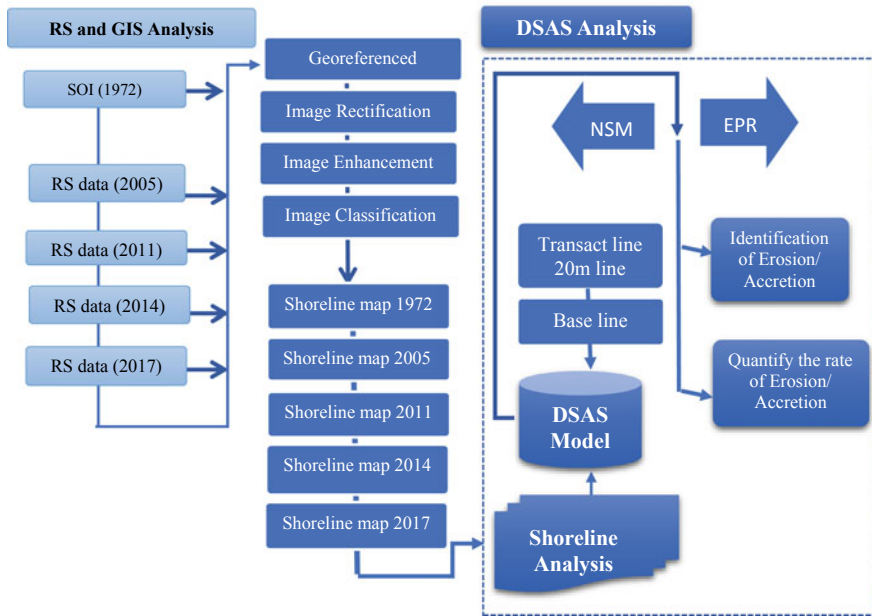


**Fig. 3** Framework of the study

**Table 2** Net shoreline movement rate 1972–2017

Year	Length in sq km			
	1973–2005	2005–2011	2011–2014	2014–2017
Erosion	– 6.0	– 0.2	– 1.7	– 0.6
Accretion	53.9	38.7	1.2	2.8

by the time elapsed between the two. Table 2 represents the shoreline classification of the study (EPR).

## 4 Results and Discussion

As Complex morphodynamic process operating at various spatial and temporal scales influence the coastal processess like erosion and accretion [17, 18]. Additional factors such as sediment availability and human interventions can influence the exact response of a coast [19, 20]. Calculation of shoreline change and sediment distribution are the methodology used for the study. Fig. 4 shows the shoreline maps derived from the SOI and remote sensing data for the years 1972–2017, and for the

same NSM and EPR, measurements were estimated to calculate the rate of erosion and accretion from 1972 to 2017 (Fig. 4).

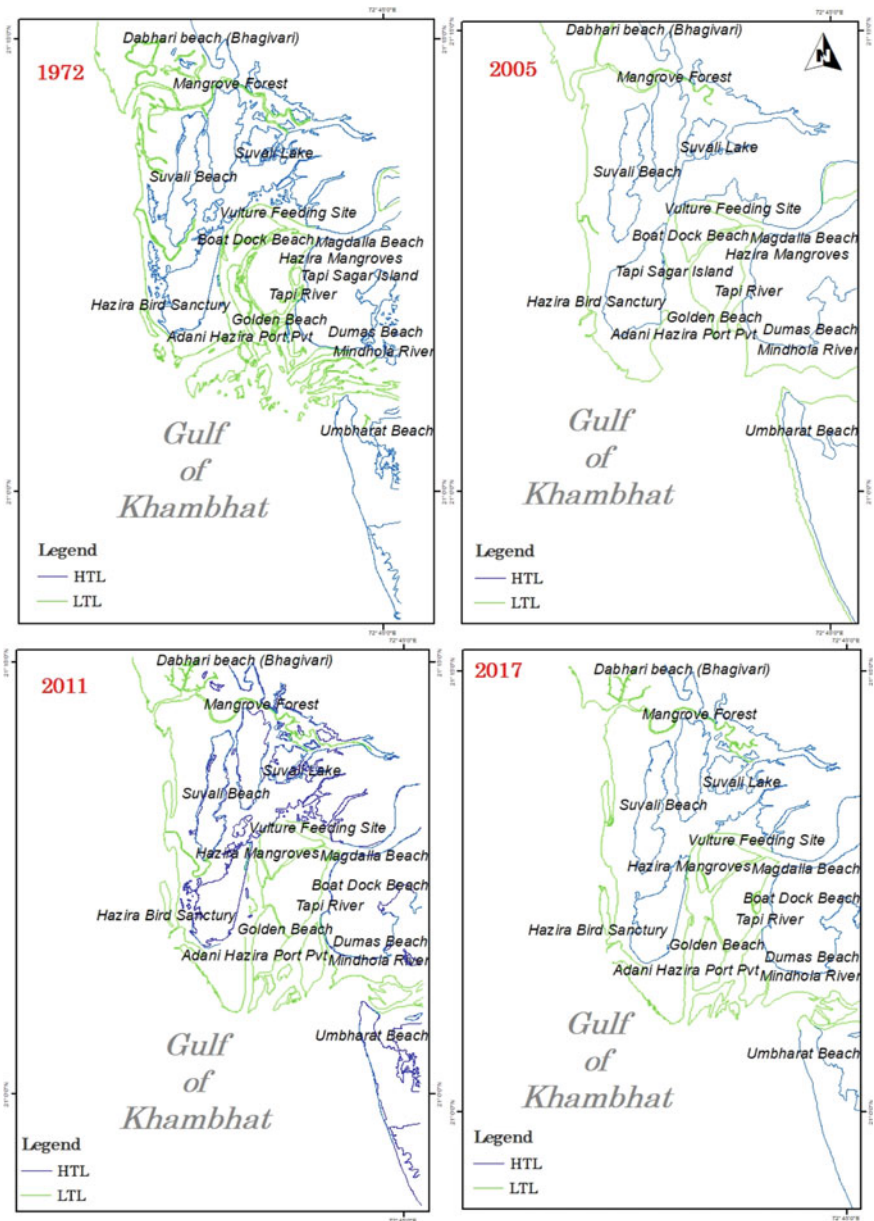
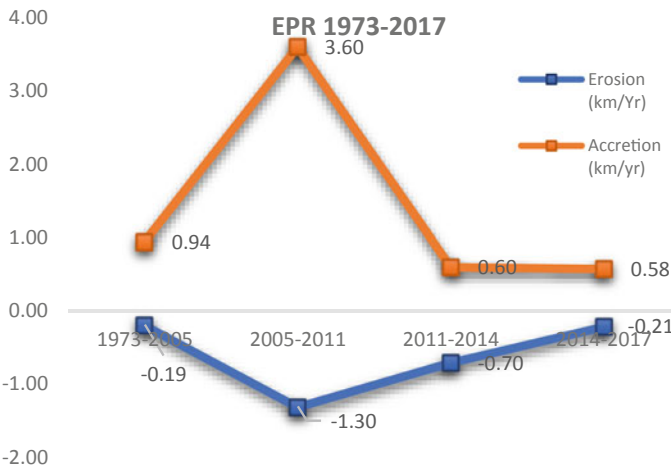
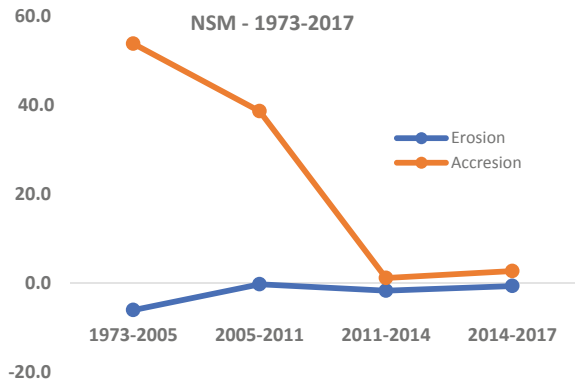


Fig. 4 HTL and LTL lines for the year 1972, 2005, 2011 & 2017

NSM studies on shoreline changes for the Tapi River Coast are shown in (Table 2 and Chart 1). Transport of sediment: According to the findings of the NSM study, the accretion rate is greater than the erosion rate. Between 1973 and 2005, erosion and accretion were approximately 0.6 km and 53.9 km, respectively. From 2005 to 2011, the erosion rate was 0.2, with an accretion of 38.7 km. For the years 2011 to 2014, erosion and accretion had no notable values; both rates were 2 km. For the years 2014–2017, erosion and accretion are approximately 0.6 km and 2.8 km (Chart 2 and Table 3).

Hydrodynamic processes like wave energy, wave direction, tidal fluctuation, and littoral currents have an impact on coastal erosion and the accretion of land-form features like beaches, beach ridges, sand dunes, and estuaries. In addition, bathymetry, coastal slope, sea-level variation, and coastal artificial constructions all play a significant role in the pace of change. The research area’s primary portions

**Chart 1** NSM for the year 1973-2017



**Chart 2** EPR for the year 1973 -2017



**Table 3** Represents the EPR rates for the year 1972-2017

Year	Erosion (km/Yr)	Accretion (km/yr)	Maximum (km/yr)	Minimum (km/yr)
1973–2005	– 0.19	0.94	0.01	– 0.01
2005–2011	– 1.30	3.60	0.06	– 0.03
2011–2014	– 0.70	0.60	0.05	– 0.07
2014–2017	– 0.21	0.58	0.04	– 0.03

are seen to have extremely variable erosion and accretion characteristics. It displays changes in coastal dynamics on both a long-term and short-term scale [16]. Parallel to the Tapi Sagar Island (Fig. 5a) near Duma and golden Beach areas Kadifalla (Fig. 5b), erosion is high for the year 2011 compared to other years. While moving toward north near Magdalla Beach, Boat Doak beach (Fig. 5d) erosion is high for the year 2014. In 2017, there was a lot of erosion around the Tapi River mouth (Fig. 5e). In the year 2011, there was significant erosion up to 500 m from the Kandifella coastal settlement area, and 400 m beyond that there was accretion. It is noticeable between the years of 2011 and 2015, when up to 300 m of erosion at the southern end of Boat Dock Beach occurred. After that, 500 m of erosion occurred again (Fig. 5d). In comparison with the previous years, erosion is seen practically across a stretch of about 400 m along the northern and southern parts of Dumas Beach (Fig. 5c). Between 2005 and 2011, there was a rate of accretion at a lower level. Accretion was slow in process between 2005 and 2011 at a rate of 9.5 km, and high accretion was observed between 1973 and 2005 and 2005 to 2011 at 15.6 km and 8.6 km, respectively. Additionally, during the year 2017, accretion was discovered for around 400 m in a deeper fashion in the area north of Boat Duck Beach (Fig. 5d). The erosion effect of sea-level rise was expounded. The main advantage of Bruun Rule is that it provides a mechanism for obtaining quantitative estimates for erosion induced by past, present, and future sea-level rise. For the practical application of Bruun Rule, determination of the appropriate limit of exchange depth and its offshore extent is one of the most perplexing problems, suggested that a typical for limiting depth for active transport of the eroded material offshore by wave action would be between 13 and 18 m. Further, he recommended that it is possible to evaluate the outer limit of exchange of beach material from sedimentological investigation, indicating the decrease in sediment size toward offshore side [21].

According to EPR findings, the erosion rate (– 1.30 km/year) and accretion rate (3.60 km/year) between 2005 and 2011 are higher than in preceding years. The rate of erosion is slightly higher for the years 2005 to 2011 (– 1.30 km/year), and then, it falls to – 0.7 km/year (2011–2014) and – 10.2 km/year after that (2014–2017). Results of accumulation show that the rate was high, with a value of 3.6 km/year, for the years 2005–2011. Then, it displays a declining tendency for the years 2011–2014 and 2014–2017, with a value of 0.6 km/year.

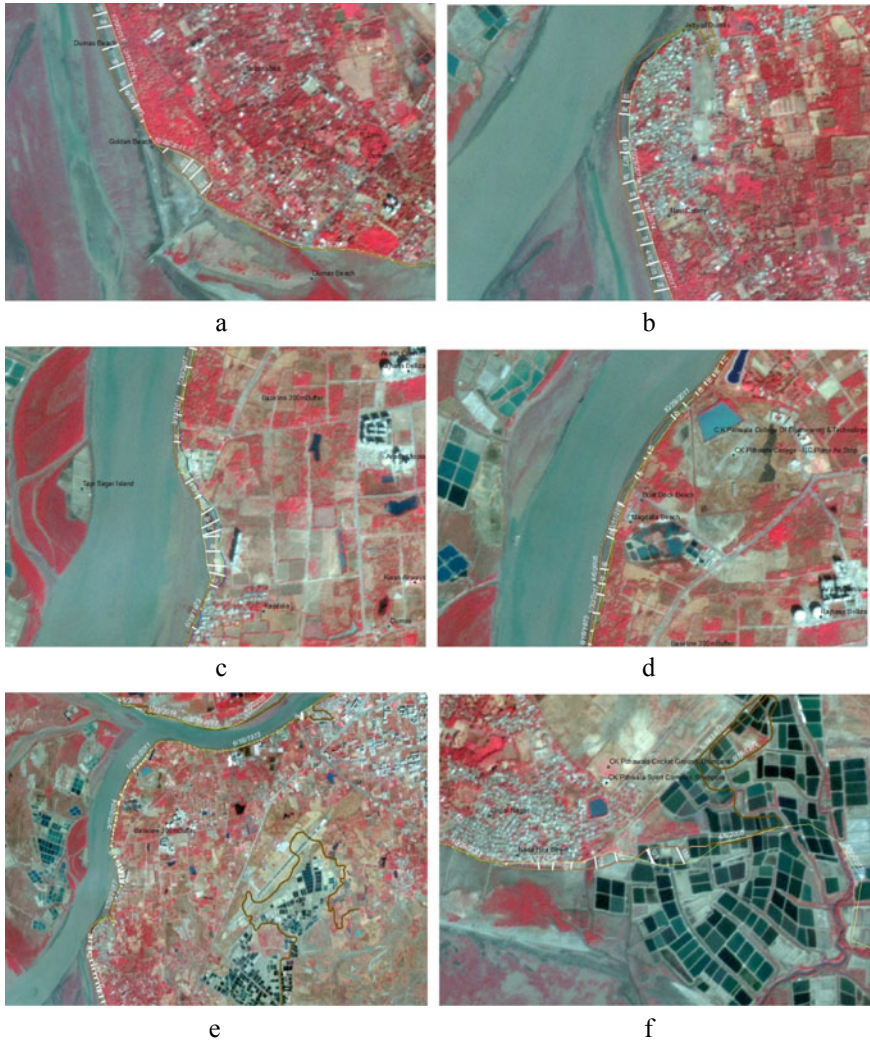


Fig. 5 Zoomed portion of the erosion and accretion area

## 5 Conclusions

According to the research of shoreline change evaluation utilizing remote sensing techniques, the study area between 1973 and 2017 saw high rates of accretion relative to erosion. The sediment distribution pattern along the Tapi River is primarily due to natural and anthropogenic factors. For evaluating shoreline change and observing specific damaged locations in smaller areas, DSAS performs well. However, the most recent methods of remote sensing with geographic information systems (GIS) have

shown to be much more efficient than traditional methods in terms of both cost and time in monitoring changes to coastlines.

## References

1. (2022). Retrieved from EOS: <https://eos.com/find-satellite/landsat-7/>
2. Benumof BT, SC (2000) The relationship between incident wave energy and seacliff erosion rates: San Diego County, rates: San Diego Country. *J Coast Res* 16(4)
3. Bruun P (1962) Sea level rise as a cause of shore erosion. *J. Waterways and Harbors Div. Proc Amer Soc Civil Eng* 88:117–130
4. Chauhan P, NS (1996) Remote sensing of suspended sediments along the Tamil. *J Ind Soc Remote Sens* 24(3):105–114
5. De Vriend H (1991) Mathematical modeling and largescale coastal behavior. Part 1: physical processes. *J Hydralic Res* 29:727–740
6. De Vriend H (1991) Mathematical modeling and largescale coastal behavior. Part 2—predictive models. *J Hydralic Res* 29:741–753
7. Dean R, Houston J (2016) Determining shoreline response to sea level rise. *Coast Eng* (114):1–8
8. Dewidar KM, FO (2010) Automated techniques for quantification of beach change rates using Landsat series along the North-eastern Nile delta, Egypt. *J Oceanogr Mar Sci* 2:28–39
9. El Asmar HM, HM (2011) Change detection of the coastal zone east of the Nile Delta using remote sensing. *Environ Earth Sci* 62:769–777
10. Himmelstoss EA, RE (2018) Digital shoreline analysis system (DSAS) version 5.0 user guide. USGS Publications Warehouse. <https://doi.org/10.3133/ofr20181179>
11. Georgiou IY, SJ (2009) Wave forecasting and longshore sediment transport gradients along a transgressive barrier island:Chandeleur Islands, Louisiana. *Geo-Mar Lett* 29:467–476
12. <https://eos.com/find-satellite/landsat-7/> (2022) Retrieved from EOS: <https://eos.com/find-satellite/landsat-7/>
13. Kaliraj S, SA (2013) Impacts of wave energy and littoral currents on shoreline erosion/accretion along the south-west coast of Kanyakumari, Tamil Nadu using DSAS and geospatial technology. *Environ Earth Sci* 71. <https://doi.org/10.1007/s12665-013-2845-6>
14. Nassar K, E-A A (2022) Quantitative appraisal of naturalistic/anthropic shoreline shifts for Hurghada: Egypt. *Mar Georesour Geotechnol* 40(5):573–588. <https://doi.org/10.1080/1064119X.2021.1918807>
15. Kiran P (2022) Paper II. In: prakashan K (ed) UPSC, p 56. [www.kiranbooks.com](http://www.kiranbooks.com). Retrieved from <http://currenthunt.com/2022/04/indian-coastline/>
16. Le Cozannet G, Bulteau T, Castelle B, Ranasinghe R, Woppelmann G, Rohmer J, Bernon N, Idier D, Louisor J, Salas-y-Mélie D (2019) Quantify uncertainties of sandy shoreline change projections as sea level rises. *Sci Rep* (9):42
17. ME H (2011) Mapping coastal erosion at the Nile Delta western promontory using Landsat imagery. *Environ Earth Sci* 64:1117–1125
18. Sheik M, CN (2011) A shoreline change analysis along the coast between Kanyakumari and Tuticorin, India, using digital shoreline analysis system. *Geo-spatial Inf Sci* 14(4):282–293
19. Nayak RA (2003) Tides in the Gulf of Khambhat, west coast of India. *Estuar Coast Shelf Sci* 57:249–254. [https://doi.org/10.1016/S0272-7714\(02\)00349-9](https://doi.org/10.1016/S0272-7714(02)00349-9)
20. Ryabchuk D, SM (2012) Long term and short term coastal line changes of the Eastern Gulf of Finland. *J Coast Conserv* 16:233–242
21. Saravanan S, CN (2011) An overview of beach morphodynamic classification along the beaches between Ovari and Kanyakumari, Southern Tamil Nadu coast. India. *Phys Oceanogr* 21(2):130–141

22. Kaaliraj S, DA (2012) Geo-processing model on Coastal vulnerability index to explore risk zone along the South West coast of Tamilnadu, India. *Int J Earth Sci Eng* 5:1138–1147. Retrieved from [https://www.researchgate.net/publication/312446890\\_Geo-processing\\_model\\_on\\_Coastal\\_vulnerability\\_index\\_to\\_explore\\_risk\\_zone\\_along\\_the\\_South\\_West\\_coast\\_of\\_Tamilnadu\\_India/citation/download](https://www.researchgate.net/publication/312446890_Geo-processing_model_on_Coastal_vulnerability_index_to_explore_risk_zone_along_the_South_West_coast_of_Tamilnadu_India/citation/download)
23. Seenipandi, DC (2012) Geo-processing model on Coastal vulnerability index to explore risk zone along the South West coast of Tamilnadu, India. *Int J Earth Sci Eng* 5:1138–1147. Retrieved from [https://www.researchgate.net/publication/312446890\\_Geo-processing\\_model\\_on\\_Coastal\\_vulnerability\\_index\\_to\\_explore\\_risk\\_zone\\_along\\_the\\_South\\_West\\_coast\\_of\\_Tamilnadu\\_India/citation/download](https://www.researchgate.net/publication/312446890_Geo-processing_model_on_Coastal_vulnerability_index_to_explore_risk_zone_along_the_South_West_coast_of_Tamilnadu_India/citation/download)
24. Thomas M, Lillesand RW (2017) *Remote sensing and image interpretation*. Wiley, Incorporated
25. White K, EA (1999) Monitoring changing position of. *Geomorphol* 29:93–105